

# Optimization of Energetic Refurbishment Roadmaps for Multi-Family Buildings utilizing Heat Pumps

Raphael Vollmer<sup>\*,1</sup>; Manuel Lämmle<sup>1,2</sup>; Stefan Hess<sup>1</sup>; Hans-Martin Henning<sup>2,1</sup>

<sup>1</sup>Albert-Ludwigs Universität Freiburg, Department of Sustainable Systems Engineering INATECH, Germany

<sup>2</sup>Fraunhofer Institute for Solar Energy Systems ISE, Germany

Preprint as published in Energy and Buildings, 2022

<https://doi.org/10.1016/j.enbuild.2022.112729>

---

## Abstract

A novel methodology for calculating optimized refurbishment roadmaps is developed in this paper. The aim of the roadmaps is to determine when and how should which component of the building envelope and heat generation system be refurbished to achieve the lowest net present value. The integrated optimization approach couples a particle swarm optimization algorithm to a dynamic building simulation of the building envelope and the heat supply system. Due to a free selection of implementation times and refurbishment depth, the optimization method achieves the lowest net present value and high CO<sub>2</sub> reduction and is therefore an important contribution to achieve climate neutrality in the building stock.

The method is exemplarily applied to a multi-family house built in 1970. In comparison to a standard refurbishment roadmap, cost savings of 6-16 % and CO<sub>2</sub> savings of 6-59 % are possible. The sensitivity of the refurbishment roadmap measures is analyzed on the basis of a parametric analysis. Robust optimization results are obtained with a mean refurbishment level of approx. 50 kWh/m<sup>2</sup>/a of the building envelope. The preferred heat generation system is a bivalent brine-heat pump system with a share of 70 % of the heat load being covered by the electric heat pump.

*Keywords: Building simulation, energetic refurbishment, particle swarm optimization*

---

## 1. Introduction

### 1.1. Motivation

The reduction of greenhouse gas emissions is the main goal regarding climate change mitigation. In this context, renewable energy technologies such as solar and wind power will play a key role in the future energy supply. Due to the increasing substitution of fossil energy sources with fluctuating renewable energy sources, flexible sector coupling technologies will be increasingly required. In the transport sector, this task can be taken over by electric vehicles; in the building sector by the electrically driven heat pump [1].

\* Corresponding author at: Albert-Ludwigs Universität Freiburg, Department of Sustainable Systems Engineering, Emmy-Noether Str. 2, 79110 Freiburg  
E-mail address: raphael.vollmer@inatech.uni-freiburg.de

Heat pumps (HP) offer ecological benefits with reduced CO<sub>2</sub> emissions as well as economic advantages compared to conventional heat supply technologies by utilizing low-temperature environmental heat sources. In Germany, for example, a total of two million heat pumps are expected to be newly installed by 2030 and respectively four million by 2050 [6]. However, to achieve the climate targets with a CO<sub>2</sub> reduction of 95 % compared to the year 1990, about 14 million heat pumps will be needed [6]. Similar statements are provided by various other studies, such as [1] or [7]. In addition to the decarbonization and flexibilization of the heat supply, a reduction of the building's heat demand is also required. For this purpose, the majority of existing buildings must be refurbished energetically to achieve an insulation standard in the range of approx. 45 kWh/m<sup>2</sup>/a [8]. For the entire building sector as such, the target states to achieve the climate goal are known. However, this is not the case at the scale of the individual building, where the cost-optimal way to achieve the climate goals is unknown - i.e. the refurbishment roadmap. Refurbishment roadmaps outline all required measures at the building envelope and heat supply, as well as the timeframe for implementation. In the context of optimized renovation roadmaps, the role of heat pumps in the refurbishment process will be investigated in particular.

### *1.2. State of research*

In the literature, mainly the final optimal energetic refurbishment of buildings has been investigated without a chronological sequence of the single refurbishment steps. Table 1 summarizes the publications that are considered relevant for a better overview of the state of the art. The key literature is classified into the following three categories depending on their optimization target.

#### *Optimization of the composition of refurbishment packages (Category A)*

The objective of this category is the identification of an optimized combination of refurbishment measures of a building for a specific point in time, for example, the optimal thickness of the building insulation, which minimizes the cumulative energy cost savings and energy-related additional costs. The range of options presented in the literature for determining appropriate retrofit packages ranges from variation-based approaches (see [12–16]) to optimization-based options. These can be further divided into building and system simulations, which are based on energy balancing approaches (see [17–23]) and thermal building models (see [24–28]), respectively. As a reference for an optimization-based approach, the work of Diakaki et al. [20] can be cited. In this case, there are no predefined packages. Instead, the generation of cost-optimal refurbishment packages for the building envelope (door, window, wall, ceiling) of a single-family home is part of the solution. Overall, it is a multi-objective optimization with a combined target function of primary energy, costs and CO<sub>2</sub> emissions.

#### *Optimization of the implementation date for predefined refurbishment packages (Category B)*

In the process of finding the optimal time for the refurbishment, time-dependent influences such as the development of energy prices, pricing of CO<sub>2</sub> emissions or inflation and interest factors of the dynamic

investment calculation play a significant factor. The goal of this classification of analysis is to calculate the ideal point in time for a refurbishment to achieve the lowest possible emissions or costs. Cypra [29] and [30] serve as a typical example for this category. Cypra determined, for example, the most suitable refurbishment packages along with the optimal timing for the one-time implementation of these measures under different boundary conditions, such as a CO<sub>2</sub> emission limit. The packages are predefined and consist of an optional building envelope refurbishment with several refurbishment stages, as well as a heat supply refurbishment using different heating technologies (gas, oil, wood pellet, heat pump). The optimization in terms of maximizing the net present value is carried out from the perspective of owner-occupiers and is applied to two single-family houses.

*Optimization of a refurbishment roadmap with defined refurbishment step sequences (Category C)*

Fully optimized refurbishment roadmaps require an "optimization of the composition of the refurbishment package" in addition to the "optimization of the implementation time", over a defined period of time.

The individual refurbishment roadmap in [31] is the most prominent example, which features the development of a refurbishment strategy under the guidance of an energy consultant. The refurbishment plan provides an initial orientation for the owner of the building, with regard to the processes and timing for the implementation of the refurbishment measures, as well as their costs. Through a planned step-by-step approach, synergies can be exploited by forming packages of measures and counterproductive actions can be avoided. However, the measures, as well as the implementation dates and costs, are kept vague and are based on the assessment and knowledge of the energy consultant. Thus, there is no proof or justification for whether the right packages are formed and whether they are implemented in the right order and at the right time. The disadvantages of this approach could be addressed by a more systematic comparison of variants or with the help of an optimization algorithm, as partly implemented by Hoier and Erhorn [32] or Nymoer et al. [33]. However, these approaches either lack central information for the comprehensibility of the results or are subject to strong simplifications, such as the energy demand calculation by using energy balance approaches instead of thermal building models.

Table 1: Selected and grouped literature concerning energetic building refurbishment depending on the optimization target and algorithm as well as complexity of building energy demand calculation, time sequence of measures, main evaluation parameters and whether heat pumps are taken into account

Paper	Target parameter		Optimization algorithm	Building and system simulations		Time sequence considered	Target function			HP considered	
	Refurbishment package	Refurbishment timing		Energetic balancing	Thermal models		costs <sup>1)</sup>	energy / CO <sub>2</sub> <sup>1)</sup>	costs and energy <sup>2)</sup>		
<b>Optimization of the composition of refurbishment packages (Category A)</b>											
Verbeeck and Hens (2005)	[12]	o/x	o	o	x	o	o	x	x	o/x	x
Kah and Feist (2005)	[13]	o/x	o	o	x	o	o	o/x	o/x	o/x	o
Enseling and Hinz (2008)	[14]	o/x	o	o	x	o	o	x	o	o/x	o
Enseling et al. (2013)	[15]	o/x	o	o	x	o	o	x	o	o	o
Almeida and Ferreira (2017)	[16]	o/x	o	o	x	o	o	x	x	x	x
Gustafsson (1998a, 1998b)	[17,18]	x	o	MILP	x	o	o/x	x	o	o	x
Pernodet et al. (2009)	[19]	x	o	GA	x	o	o	x	x	o/x	o
Diakaki et al. (2010)	[20]	x	o	CP	x	o	o	x	x	o	o
Fan and Xia (2015, 2017)	[21,22]	x	o	MINLP/ GA	x	o	o	o	o	x	o
Kunze (2016)	[23]	x	o	CPLEX	x	o	o	x	x	o	x
Peippo et al. (1999)	[24]	x	o	PS	o	o/x	o	x	x	o/x	o
Nielsen (2003)	[25]	x	o	DSA	o	o/x	o/x	x	o	o	o
Almeida and Freitas (2013)	[26]	x	o	NSGA-II	o	o/x	o	x	o/x	o	o
Asadi et al. (2014)	[27]	x	o	GA	o	o/x	o	x	x	o/x	x
Shadram et al. (2020)	[28]	x	o	GA	o	x	o	o	x	o	o
<b>Optimization of the implementation date for predefined refurbishment packages (Category B)</b>											
Cypra (2010)	[29]	o/x	o/x	CPLEX	x	o	o	x	o	o	x
Kumaroglu and Madlener (2012)	[30]	o/x	o/x	o	n. s.	n. s.	o	x	o	o	x
<b>Optimization of a refurbishment roadmap with defined refurbishment step sequences (Category C)</b>											
Hoier and Erhorn (2013)	[32]	o/x	o/x	o	x	o	x	o	x	o	x
Dena (2020)	[31]	o/x	o/x	o	x	o	x	o	o	o/x	x
Nymoer et al. (2021)	[33]	x	x	n. s.	x	o	x	o	o	x	x

x = yes  
 o = no  
 o/x = valid under certain boundary conditions / restrictions  
 n. s. = not specified  
 CP = Compromise programming  
 CPLEX = Optimization software package with simplex method  
 DSA = Direct search simulated annealing  
 GA = Genetic algorithm  
<sup>1)</sup> = independent consideration of costs or energy  
<sup>2)</sup> = multi-criteria optimization of costs and energy  
 MILP = Mixed-integer linear programming  
 MINLP = Mixed-integer nonlinear programming  
 NSGA-II = Non-dominated sorting genetic algorithm

### 1.3. Novelty and scientific contribution

Concluding from the state of research, the individual components of a refurbishment roadmap have already been investigated and described in various papers. However, only individual aspects are examined in all known publications. In case of category A, the time dimension is missing and the focus is usually placed on the economic analysis. Technical interactions such as those between the building envelope and the heat supply are neglected. In the case of category B, the initial building conditions are only taken into account to a very limited extent and refurbishment packages are already predefined. The publications in category C are either based on the subjective assessment of energy consultants or on approximate estimates without the integration of objective and optimized calculation algorithms [31].

The novelty of this work consists of the development of a methodology for the optimization of individual energetic refurbishment roadmaps for multi-family buildings. The central research question is:

*When and how should which building or heat supply system component be refurbished in order to achieve the best possible heat supply in terms of costs or CO<sub>2</sub>-emissions?*

The method takes a new holistic approach to the refurbishment process by optimizing not only the scope of the refurbishment measures but also the timing of their implementation. For this purpose, a thermal building simulation is coupled with an optimization algorithm. A key novelty is the possibility to use heat pumps in the context of refurbishment roadmaps for multi-family houses. Due to the fact that the efficiency of the heat pump is strongly dependent on the source and sink temperature levels, a detailed and technically accurate simulation of the heat supply system is required. This is especially valid in the context of refurbishment roadmaps, where small calculation errors can quickly add up to relevant discrepancies due to the long observation period. Furthermore, the influence of boundary and initial conditions is investigated in the context of robustness tests. From this, conclusions can be drawn regarding the influence of factors such as energy and CO<sub>2</sub> prices, subsidies, building geometries, building age classes, etc. on the course of the refurbishment roadmaps.

In the later course of this paper, section 2 presents the methodological approach for calculating the individual refurbishment roadmaps. The reference building on which the results are based is described in section 3. The methodology is applied under varying boundary and initial conditions in section 4, followed by a discussion of the results in section 5. Section 6 concludes the paper with a summary.

## 2. Optimization methodology for renovation roadmaps

In the following, the methodology for determining optimized refurbishment roadmaps optRR is explained. The new optimization method, which can be classified into the previous classification C, considers the following requirements:

- Temporal perspective over a predefined period of time and individual initial conditions of the buildings
- Search for suitable refurbishment measures in a solution space that is as large as possible and technically feasible at the same time
- Flexible implementation dates for refurbishment measures without a fixed coupling to technical component lifetimes
- Technical interactions between refurbishment measures and heat supply technologies are taken into account, as well as the related aspects with regard to system efficiency
- Inclusion of economic aspects such as capital interest rates, energy cost developments and ecological constraints such as CO<sub>2</sub> pricing
- Flexible targets can be set, such as upper limits for CO<sub>2</sub> emissions.

The presented approach is of a generic nature, implemented in MATLAB and can be applied to any type and size of residential building, as long as all the required boundary conditions are known. As shown in Figure 1, the methodology is divided into three main parts: thermal building simulation, economic efficiency calculation and mathematical optimization.

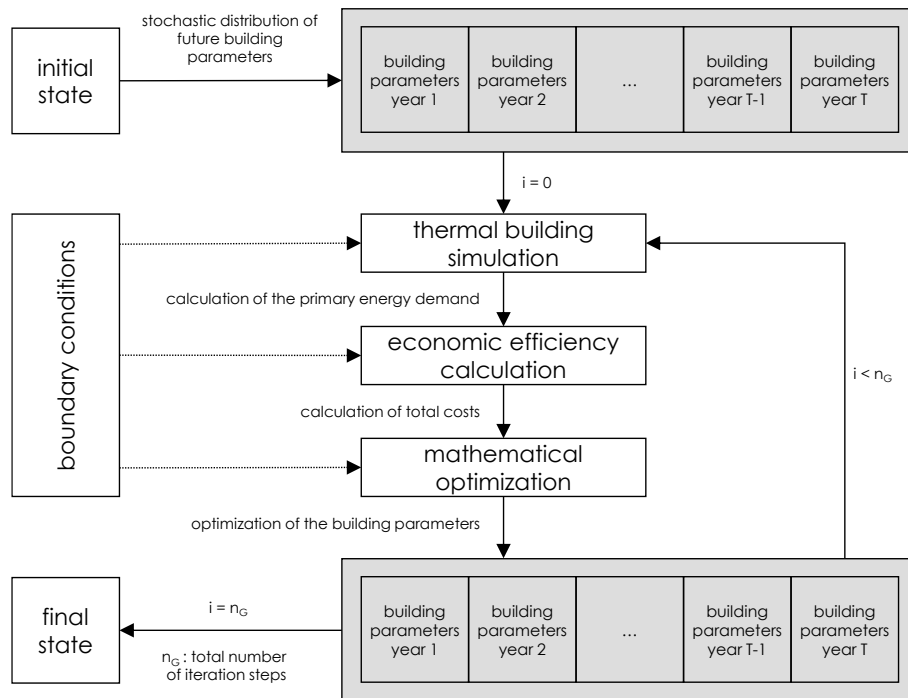


Figure 1: Generic methodology for determining optimized refurbishment roadmaps

The starting position for every refurbishment roadmap is the building-specific initial state, which forms the basis for all refurbishment decisions regarding the depth of refurbishment and the time of implementation.

The initial state is characterized by the following parameters:

- Geometric building dimensions
- Building structure with thermal characteristics and age of components
- Heat supply systems for space heating and domestic hot water with installation times
- Number of occupants or details of previous energy consumption

Based on this information, a first proposal is made for the building-specific refurbishment roadmap for the time period  $T$ . In this proposal, the building optimization parameters are defined for each year. For example, the thermal properties of the building envelope or the type and output of the heat generation system. The building simulation is used to calculate the energy demand. Together with the investment and maintenance costs, the determined energy demand is an input variable for the dynamic economic efficiency calculation. The following optimization minimizes the determined net present value (NPV), which thus represents the objective function. For this purpose, the parameters released for the optimization are varied according to the optimization algorithm in Eq. (3). The final state after  $n_G$  iterations contains a specific value for each optimization parameter and for each individual year in the period under consideration.

Figure 2 extends the approach for determining the optimized refurbishment by its central technical components, in particular concerning the thermal building simulation. For simplicity, the graphic is reduced to the logical procedure and workflow of the individual parts of the methodology. The parts belonging to the optimization are marked in green and are recalculated in each iteration. This includes the actual optimizer (here: particle swarm optimization) as well as the models and subroutines of the building and heat generators influenced by the optimization parameters. The black dashed elements remain constant and are calculated initially. This includes the domestic hot water (DHW) calculation with the fresh water station, storage and controller, the dimensioning of the radiators for space heating (SH), as well as the irradiation calculation.

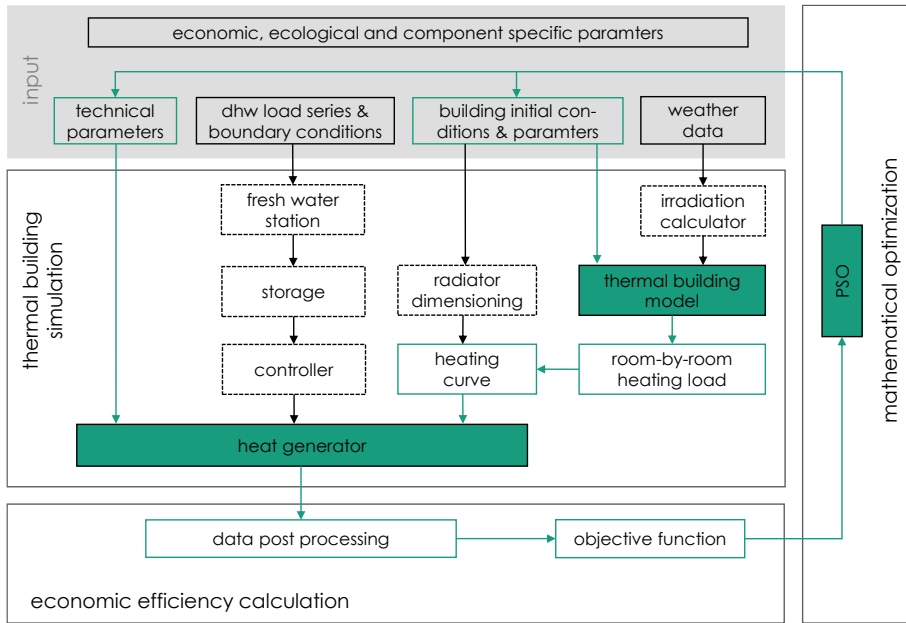


Figure 2: Simplified representation of the optRR methodology with used subroutines and sequential processes

### 2.1. Coupled dynamic thermal building model and system simulation

The thermal building model calculates the energy required for space heating and domestic hot water. Figure 3 shows a schematic hydraulic representation of the heat flow between the energy source and heat demand in the context of a building heat supply system. While the SH demand is determined using a dynamic thermal building simulation model, the DHW demand is specified by a load series generated with the software synPRO [34]. Besides the HP (main generator) and gas condensing boiler (auxiliary generator), the heat supply system also consists of a separate SH and DHW storage tank, as well as a heat transfer system. The heat transfer system consists of radiators for transferring the heat to the room air and a fresh water station for transferring the heat to the DHW. In the case of a bivalent system consisting of a heat pump in combination with an auxiliary generator, the operating mode is bivalent-parallel. This means that, below a defined outdoor temperature, the auxiliary gas boiler supports the HP in parallel operation. In addition to the storage and distribution losses, dynamic system temperatures such as the heating supply temperature are also calculated. The required energy amount is finally determined by balancing the energy source for the heat generators. This allows the calculation of annual CO<sub>2</sub> emissions in addition to energy costs.

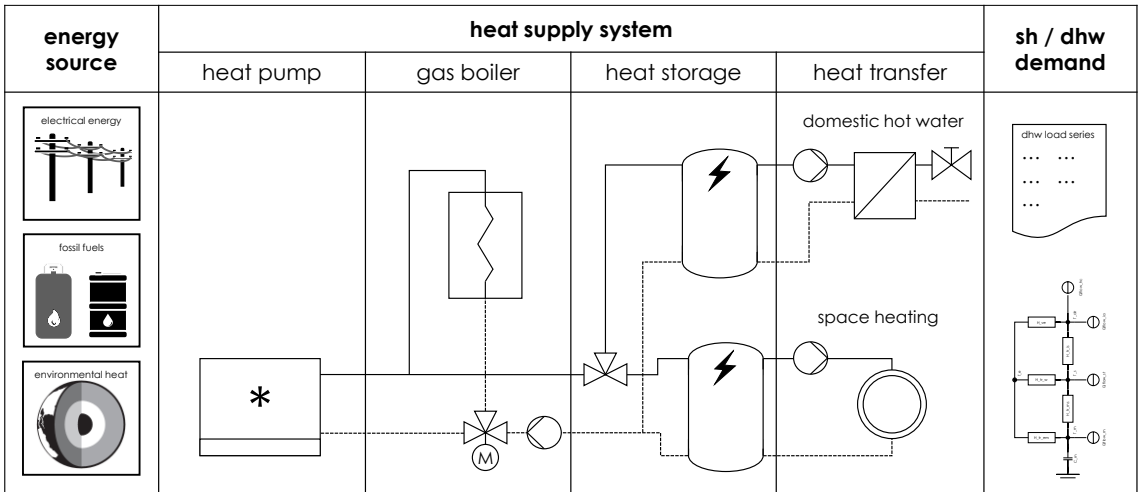


Figure 3: Coupled dynamic thermal building model with heat supply system as link between energy source and heat demand

In detail, the building modeling is implemented using a resistance-capacity 5RIC model according to DIN EN ISO 13790 [35]. The objective of the building simulation is to determine the heat demand during every hourly time step, balancing the heat losses (transmission and ventilation) and the heat gains (internal and solar). Both the heat losses and the gains depend on building physics, user-related and location-specific boundary conditions. Solar gains are calculated using the SUNAE algorithm in combination with the Temps-Coulson-Klucher approach to calculate sky diffuse radiation [36,37]. As a weather data set, the Typical Meteorological Year (TMY) of the city of Potsdam is used. The central European location has a heating-dominated climate, therefore the focus in this analysis is placed on heating and cooling is neglected. With the known nominal heat output of the installed radiators and the maximum required heat output of the thermal building simulation, the necessary temperature level of the radiators can be determined for a specific mass flow ratio. The dynamic supply and return temperatures of the heating circuit are then calculated as a function of the outdoor temperature using a heating curve [38]. The fresh water station is simplified and simulated as a heat exchanger. With reference to Figure 3, a thermal storage is included in both the SH and DHW circuits, which leads to a temporal decoupling of the heat generator and heat consumer. In the case of SH, calculations are made with one-hour step sizes due to computing capacities, which would lead to oversized storage tanks or strong temperature fluctuations. The storage losses are therefore estimated using the averaged heating circuit temperature from the supply and return flow. Since the DHW system is calculated initially, the higher computation effort due to the simulation as a stratified storage is not relevant. However, the implementation of a stratified storage tank enables a better representation of the influence of temperature spreads and high DHW temperatures and their influence on the heat pump's SCOP. The high temperatures of at least 60 °C are due to the DHW hygiene in the MFH [39]. The modeling of the 5-layer storage tank is an adaptation of Fraunhofer ISE [40–42]. The air and brine heat pump models are based on the TRNSYS model Type401. The instantaneous heating power and

coefficient of performance are represented by biquadratic polynomials [43]. The characteristic curve maps are based on manufacturer's data like [44] and [45] with a chosen maximum HP supply temperature of 62 °C. As for the gas condensing boiler, the same procedure as for the HP is chosen with biquadratic polynomials and manufacturer's data [46]. The heating power of HP and gas condensing boiler is scaled freely under the assumption of only a slightly changing performance curve. In the case of a brine HP, the borehole field is dimensioned according to VDI 4640 with a maximum length of 150 m per probe and a thermal conductivity of 2.4 W/(m<sup>2</sup>K) [47,48].

## 2.2. Economic efficiency calculation and CO<sub>2</sub> emissions

The net present value (NPV) method according to Eq. (1) is used for the economic efficiency calculation [49]. The dynamic investment calculation allows the comparison and evaluation of the different refurbishment roadmaps on a financial level. The assumed inflation rate  $r$  is 2 % [50] and the assumed interest rate  $q$  is 5 % [51]. The annual costs  $z$  ( $z_t$  at year  $t$ ) include the capital, energy and maintenance costs. The residual values ( $rv$ ) decrease linearly and are used to account for the possible discrepancy between the period under consideration and the actual period of use.

$$NPV = - \sum_{t=0}^T \frac{(1+r)^t}{(1+q)^t} \cdot z_t + \frac{(1+r)^t}{(1+q)^T} \cdot rv \quad (1)$$

The following tables in the Appendix summarize the cost functions used for the building envelope (Table 9), heat generators (Table 10), energy costs (Table 11), and CO<sub>2</sub> emission factors (Table 12). The NPV at the end of the observation period is the cost function for the optimization.

The levelized costs of heat are a more comprehensive economic indicator, which is therefore used for the latter economic assessment. It is derived from the NPV as the ratio of the net present value and the amount of heat generated  $Q_{gen,i}$  over the period under consideration  $T$ :

$$LCOH = \frac{NPV}{\sum_{j=1}^T Q_{gen,j}} \quad (2)$$

## 2.3. Mathematical optimization via particle swarm optimization

Optimization methods are divided into deterministic and stochastic methods. Deterministic methods have a consistent mathematical sequence with repeatable solutions. However, the objective function partly has to be described in a mathematically complex way and the search space is often locally limited [52]. The particle swarm optimization (PSO) method used here belongs to the stochastic, nature-inspired algorithms and imitates the swarming behavior of birds or fish. Advantages over the deterministic approach are the simple mathematical description of the objective function and the possibility to decouple the optimization from the system simulation, which results in larger degrees of freedom in the model structure [53]. A disadvantage of stochastic optimization methods is the lack of the possibility to generate repeatable solutions. Responsible for this is the random-based part, which allows an easier skipping of local optima

and thus an easier determination of the global optimum [54,55]. Mathematically, the position of a particle can be calculated as follows [56–58]:

$$\vec{x}_{i,k+1} = \vec{x}_{i,k} + \vec{v}_{i,k+1} \quad (3)$$

with the velocity vector:

$$\vec{v}_{i,k+1} = \omega_k \cdot \vec{v}_{i,k} + c_1 \cdot \vec{r}_{1,i,k} \odot (\vec{l}_{best,i,k} - \vec{x}_{i,k}) + c_2 \cdot \vec{r}_{2,i,k} \odot (\vec{g}_{best,k} - \vec{x}_{i,k}) \quad (4)$$

The velocity vector is made up of the three central properties of particle swarm optimization:

- 1) The particles have a current velocity  $\vec{v}_i$ , whose influence can be adjusted via an inertia weight  $\omega_k$  and prevents sudden velocity changes.
- 2) The particles have a local memory  $\vec{l}_{best,i}$ , in which the best condition found by the particle is stored. In addition to the stochastic influence caused by  $\vec{r}_{1,i}$ , there is a cognitive factor  $c_1$  to weight the influence and is randomly drawn between [0,1].
- 3) The particles have a global memory  $\vec{g}_{best}$  in which the best condition found by the swarm is stored. As with cognitively influenced velocity, there is a stochastic influence via  $\vec{r}_{2,i}$  with numbers randomly drawn between [0,1] and the social factor  $c_2$  for weighting.

The time-dependent weighting of  $\omega_k$ ,  $c_1$ ,  $c_2$  are calculated via the following approach – here representative with  $\omega_k$  [59,60]:

$$\omega_k = \omega_1 + \frac{k}{n_G} (\omega_2 - \omega_1) \quad (5)$$

In addition to the temporal adaptation, a success-dependent adaptation of the velocity vector according to Helwig [61] is implemented. Table 2 contains the central setting parameters for the PSO.

Table 2: Parameter settings for the particle swarm optimization

parameter	value	description
number of generations $n_G$	1500	max. number of iterations
population size $n_P$	50	number of particles
inertia weight $w_1$ and $w_2$	0.9 $\rightarrow$ 0.4	start value $\rightarrow$ end value
cognitive component $c_{1,1}$ and $c_{1,2}$	2.5 $\rightarrow$ 0.5	start value $\rightarrow$ end value
social component $c_{2,1}$ and $c_{2,2}$	0.5 $\rightarrow$ 2.5	start value $\rightarrow$ end value

#### 2.4. Main optimization parameters

The considered solution space of the PSO is presented in Table 3. The insulation thickness of the envelope components is scaled in 1 cm steps and almost meets passive house standards in the final state. The heat generators are scaled in 2.5 kW steps and can be varied from 0 to 67.5 kW. In addition to the technical components listed in Table 3, there is always a heating rod installed acting as a backup in the case of undersized heat generators. Thus, the heat demand is always met.

Table 3: Solution space considered for the optimization variables

parameter	value	unit
envelope components		
U-value window	1.9, 1.3, 1.0, 0.8	W/(m <sup>2</sup> K)
insulation thickness wall	0 to 0.24	m
insulation thickness ceiling	0 to 0.3	m
insulation thickness floor	0 to 0.3	m
insulation thickness roof	0 to 0.24	m
technical components		
heating power gas condensing boiler	0 to 67.5	kW
heating power AW/HP	0 to 67.5	kW
heating power BW/HP	0 to 67.5	kW

### 3. Description of reference multi-family building

The methodology is demonstrated using the example of a multi-family house located in Potsdam that was built in 1970 and is thus located in the range of the two construction periods with the largest stock in Germany [62]. A rendering of the building is shown in Figure 4.

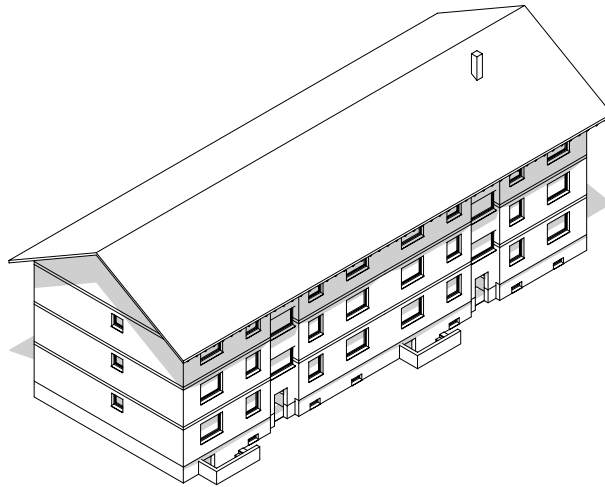


Figure 4: 3D rendering of the reference three-storey multi-family building with 12 apartments for 20 residents

Further parameters concerning the building modeling can be taken from Table 4 and Table 5:

Table 4: Dimension of the investigated multi-family building

parameter	value / comment
number of full storeys	3
number of apartments	12
number of staircases	2
cellar & attic	available and non-heated
building orientation	north-south (gable side)
building dimensions	11.9 m x 32.1 m
storey height	2.75 m
clear ceiling height	2.55 m
conditioned living space per apartment	75.7 m <sup>2</sup>
net floor space	969.5 m <sup>2</sup>

Table 5: Overview of the parameters required for the building simulation

parameter	value	source
room set point temperature	20 °C	[63]
internal heat gain	90 Wh/(m <sup>2</sup> d) <sup>a)</sup>	[63]
min. outdoor air exchange rate	0.6 h <sup>-1</sup>	[64]
number of occupants	1.7 person/WE	[65]
thermal bridge surcharge	0.1 W/(m <sup>2</sup> K)	[66]
temperature correction attic	0.8	[64]
temperature correction cellar	0.6	[64]
shading factor <sup>b)</sup>	0.1	[35]
window frame share	0.25 %	[67]
spec. heat capacity	260 kJ/(m <sup>2</sup> K) <sup>a)</sup>	[35]

a) value refers to net floor area (here: conditioned living space)  
b) permanent irradiation reduction due to internal privacy screen

An overview of the assumed initial conditions of the relevant optimization parameters is given in Table 6, including the initial states of the building envelope as well as the heat generation technology based on a gas condensing boiler. Due to the previous refurbishment stages, the original components of the windows, top floor ceiling and heat supply system have already been replaced once or insulated. In its initial state, the building has a specific heating demand of ca. 139 kWh/(m<sup>2</sup>a) with a nominal heat load of 59.2 kW and a domestic hot water demand of ca. 20 kWh/(m<sup>2</sup>a) including circulation and storage losses. The domestic hot water demand is not addressed in the optimization process and is therefore considered constant.

Table 6: Initial condition of the relevant optimization parameters in 2020

component	initial value	technical lifetime	installation date
window	1.90 W/(m <sup>2</sup> K)	30 a	2000
exterior wall	1.15 W/(m <sup>2</sup> K)	40 a	1970
top floor ceiling	0.25 W/(m <sup>2</sup> K)	60 a	2000
bottom floor	1.17 W/(m <sup>2</sup> K)	60 a	1970
roof	2.00 W/(m <sup>2</sup> K)	50 a	1970
gas condensing boiler	60 kW	20 a	2010

## 4. Results

### 4.1. Optimized refurbishment roadmap of the reference building

Figure 5 shows the results of the optRR methodology for the reference building. For this example case, a linear increase of the CO<sub>2</sub> price  $p_{\text{CO}_2}$  of 180 €/tCO<sub>2</sub> until 2050, an interest rate  $r$  of 5 % and a maximum HP supply temperature  $T_{\text{sup,max}}$  of 62 °C are assumed as the central boundary conditions.

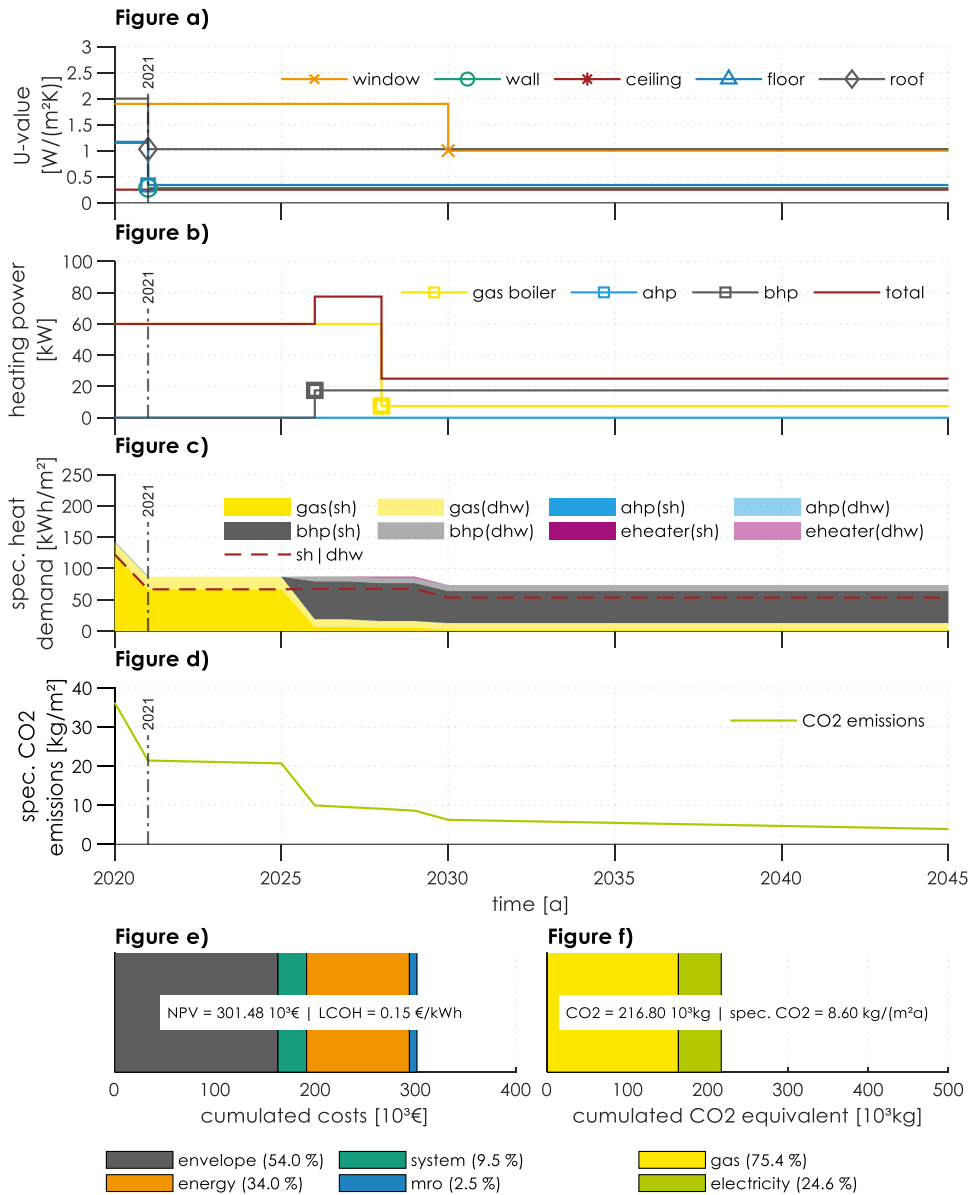


Figure 5: Optimized refurbishment roadmap for the reference building with a) U-value of building components, b) heating power of heat supply system c) specific heat demand and contributions per heat generator, d) specific CO2 emissions, e) cumulated costs (NPV) and f) cumulated equivalent CO2 emissions per energy carrier (ahp = air heat pump, bhp = brine heat pump, mro = maintenance, repair and operation cost)

The refurbishment roadmap shown in Figure 5 is one of many ways to present a refurbishment roadmap and includes the key measures and results. The figure chosen here contains six distinct sections a) through f). Each section contains different information about the identified refurbishment roadmap:

- a) Information on the refurbishment level (U-value) of the building envelope and the respective implementation dates, which are shown as symbols (cross: window, circle: wall, star: ceiling,

triangle: floor, rhombus: roof). In total, the floor (2021,  $U = 0.34 \text{ W}/(\text{m}^2\text{K})$ ), exterior wall (2021,  $U = 0.29 \text{ W}/(\text{m}^2\text{K})$ ), roof (2021,  $U = 1.03 \text{ W}/(\text{m}^2\text{K})$ ) and windows (2030,  $U = 1.0 \text{ W}/(\text{m}^2\text{K})$ ) will be refurbished in the period under consideration. It is worth mentioning that the floor is the only component that is refurbished prior to its end of lifetime.

- b) Information on the installed heating power of the different heat generators, the total installed heat generator power and the respective installation dates. The implementation date is shown as a square symbol. In the course of the refurbishment, a 17.5 kW brine HP will be installed in 2026, in addition to the existing 60 kW gas condensing boiler. The gas boiler is replaced in 2028 by a significantly smaller version with 7.5 kW. From 2030 onwards, the refurbishment of the windows reduces the heating demand and the gas boiler is primarily used for DHW generation.
- c) Visualization of the specific heat demand per square meter of conditioned building area by heat generator and space heating (dark color) respectively domestic hot water (light color). The heating demand of the building is reduced from the initial 118 kWh/(m<sup>2</sup>a) in 2020 to 53 kWh/(m<sup>2</sup>a) in 2030. The area above the dashed line represents the DHW share of all heat generators (20 kWh/(m<sup>2</sup>a) incl. circulation and storage losses).
- d) Development of the specific CO<sub>2</sub> emissions over the period under consideration. The CO<sub>2</sub> emissions decrease due to the continuously decreasing CO<sub>2</sub> emission factors of grid electricity (Table 12), the reduction of the heating demand in the course of the refurbishments and change of the emission factor from gas to electricity by installing an electric HP.
- e and f) General information regarding the costs (NPV: net present value) of 301.5 k€ and CO<sub>2</sub> emissions of 216.8 t over the entire period with a time horizon until the year 2045. The costs are broken down on a percentage basis between the investment costs (building envelope and heat generation system), energy costs and maintenance and repair costs (mro). With the specific indication of 0.15 €/kWh<sub>th</sub> (LCOH: levelized cost of heat) and 8.6 kg of CO<sub>2</sub> emissions per square meter of heated floor area, a comparison with other buildings is possible.

#### 4.2. Impact of the degrees of freedom in the search space on the results

In order to investigate the influence and added value of the optimization on the refurbishment roadmap, the degrees of freedom of the optimizers' search space are increased step by step. The degrees of freedom vary in terms of refurbishment depth and timing for the individual refurbishment roadmaps (Table 7):

- *BAU* represents the business as usual case (BAU) without any optimization. At the end of their technical lifetime, all components are replaced by building components that comply with the refurbishment level of the German Building Energy Act (GEG). Consequently, the refurbishment level, implementation time, and technology are fixed.
- *FreeSys*: the optimizer is free to choose the heat generation technology, while the refurbishment level is set to the GEG standard. The implementation date is linked to the fact that the old heat generator has reached 100 % of its technical life (100 % lifetime boundary condition). Thus, a component is only addressed when it has reached the end of its technical lifetime.
- *FreeRefurb*: the optimizer can freely choose the refurbishment level between the current state and the state of a passive house. All other optimization variables and heat supply are fixed.
- *Lifetime*: a flexible refurbishment level and a freely selectable heat supply technology with a maximum technical lifetime of the components are investigated.
- *Gas, AHP, and BHP*: not only the refurbishment level but also the refurbishment time can be selected. The heat generation is preset with gas (Gas), air-water HP (AHP) and brine-water HP (BHP).
- *optRR*: the only limitation is a minimum retention time of the component in the building of 50% of its technical service life due to ecological aspects (gray energy, etc.).

Table 7: Summary of the influence of the different degrees of freedom of the optimizer on the NPV and CO<sub>2</sub> emissions for the different cases A to H. Heat demand and size of heat generator of the year 2045 for comparison reasons.

boundary conditions				results				
case	refurb.	tech.	heat	spec. NPV [€/m <sup>2</sup> /a]	spec. CO <sub>2</sub> [kg/m <sup>2</sup> /a]	spec. heat dem. [kWh/m <sup>2</sup> /a]	heat gen.	
	level	lifetime <sup>1)</sup>	gen.				gas	hp
BAU	GEG	100 %	gas	-14.78	19.39	57.7	30	0
FreeSys	GEG	100 % <sup>2)</sup>	-	-13.32 (-9.9%)	10.68 (-44.9%)	57.9	7.5	20
FreeRefurb	-	100 %	gas	-13.96 (-5.5%)	18.27 (-5.8%)	48.8	27.5	0
Lifetime	-	100 % <sup>2)</sup>	-	-12.69 (-14.1%)	11.09 (-42.8%)	53.1	7.5	17.5
Gas	-	> 50%	gas	-13.77 (-6.8%)	16.62 (-14.3%)	48.8	25	0
AHP	-	> 50%	ahp	-13.06 (-11.6%)	9.23 (-52.4%)	52.7	0	25
BHP	-	> 50%	bhp	-12.64 (-14.5%)	8.01 (-58.7%)	53.3	0	20.0
<b>optRR</b>	-	<b>&gt;50%</b>	-	-12.44 (-15.8%)	8.94 (-53.9%)	53.3	7.5	17.5

<sup>1)</sup> percentage of technical service life that components must be installed in the building

<sup>2)</sup> 100% lifetime in combination with flexible heat generation means that the new heat generator is not installed until the old one has reached the end of its technical lifetime

The optimizer achieves the highest savings in costs and CO<sub>2</sub> in the case of the highest degree of freedom (case *optRR*). This is due to the fact that each constraint reduces the solution space and thus increases the probability that the optimizer will find only a local and not a global cost optimum. Consequently, the global optimum is reached with the highest degree of freedom. Compared to the reference case BAU, cost savings of over 15 % and CO<sub>2</sub> savings of nearly 55 % are possible. A technology change from a gas boiler to a BHP shows the greatest single effect, as shown in the case *FreeSys*. Since the GEG level covers an already very good thermal insulation standard, there is no major effect of the optimizer here. The savings shown in the case *FreeRefurb* are mainly based on the better price-performance ratio of the improved windows compared to the GEG standard (U-value 1.0 instead of 1.3 W/m<sup>2</sup>/K), floor (U-value 0.25 instead of 0.32 W/m<sup>2</sup>/K) and a worse insulated roof (U-value 1.04 instead of 0.26 W/m<sup>2</sup>/K). A free choice of the implementation date even before the end of the technical service life enables further savings in costs and CO<sub>2</sub> emissions. In the case *Gas*, the bottom floor is insulated ahead of schedule. The residual value of envelope components is negatively added to the NPV due to the value loss. If the saved energy costs compensate for the linearly assumed residual value costs, the refurbishment is carried out ahead of schedule. The case *Lifetime* corresponds to a common situation, where refurbishments are often carried out only when a component fails. However, due to the replacement intervals dictated by technical service life, cost-saving measures such as early heat pump installation or early floor insulation are overlooked. The cases *AHP* and *BHP* are designed as mono-energetic systems and have a similar refurbishment level compared to the case *Gas*. The switch to electricity as an energy source enables the largest CO<sub>2</sub> savings. The high CO<sub>2</sub> savings in the case of the heat pump are due to the high energy efficiency by leveraging ambient heat sources, resulting in a COP > 1. Secondly, the CO<sub>2</sub> factor of electricity is expected to decrease with the future transition of electricity generation from fossil to renewable sources, from ca. 403 g/kWh in 2020 to ca. 21 g/kWh in 2050, compared to the almost unchanged CO<sub>2</sub> factor of gas from ca. 200 g/kWh in 2020 to ca. 166 g/kWh in 2050 (cf. Table 12).

The cases shown in Table 7 underline both the basic suitability of the optimizer for finding improved refurbishment roadmaps and the added value of applying optimization methods with a wide search space in generating these roadmaps. The achieved savings correlate with the number of degrees of freedom of the optimizer. Accordingly, higher costs must be accepted if only partial aspects regarding refurbishment level, heating technologies and timing are optimized.

#### 4.3. Robustness of refurbishment roadmaps concerning boundary conditions

After introducing the basic functionality in the previous sections, the sensitivity of selected parameters on the refurbishment roadmap is analyzed in the following. The optimized case *optRR* is used as the initial scenario (CO<sub>2</sub> price  $p_{CO_2} = 180$  €/tCO<sub>2</sub>, no subsidy, interest rate  $r = 5$  %, max. HP supply temperature  $T_{HP} = 62$  °C).

As a first parameter, the CO<sub>2</sub> prices included in the energy prices are varied (cf. Table 11). In addition to the already used case with a linear increase of 180 €/tCO<sub>2</sub> until 2050, the extreme cases without a CO<sub>2</sub> price (0 €/tCO<sub>2</sub>) and with a high CO<sub>2</sub> price (260 €/tCO<sub>2</sub>) are analyzed. Table 8 shows that the CO<sub>2</sub> pricing has no influence on the insulation standard and only a very small effect on the specific NPV, but leads to an earlier installation of a larger BHP. This results in a greenhouse gas reduction of 20.5 % (180 €/tCO<sub>2</sub>) compared to the case without any CO<sub>2</sub> price (0 €/tCO<sub>2</sub>). An increase in the CO<sub>2</sub> price from 180 € to 260 € by 2050 leads to an even earlier installation of the HP and consequently, to further emission savings in the studied case.

Another heavily politically influenced factor are subsidies for heat supply systems and refurbishments (*Subsidy*). The assumed values of the model correspond to the subsidies valid in Germany. These vary between 20 % for the building envelope, 30 % for a bivalent and 35 % for a mono-energetic system. In combination with a refurbishment roadmap, an additional 5 % is possible [68]. The subsidies lead to significant savings in the net present value (17.0 %). On the system side, the cost reduction enables an earlier installation of a larger HP. This causes a reduction in CO<sub>2</sub> emissions of 14.4 % compared to the reference case optRR. The subsidies have only a small effect on the envelope refurbishment, as can be seen in Table 8.

As a third parameter, the interest rate is varied. In addition to the average interest rate of  $r = 5\%$  chosen so far, a low interest rate of  $r = 3\%$  ( $IR=3\%$ ) and a high interest rate of  $r = 7\%$  ( $IR=7\%$ ) are also considered. By increasing the interest rate, the costs for refurbishment and operation decrease (cf. Table 8). This is due to the method of calculating the NPV, in which the expenses are discounted to the current point in time by the discount factor influenced by the interest rate. Consequently, the investment timing shifts to a later point in time. The system composition and the refurbishment standards barely change. Thus, the CO<sub>2</sub> savings at lower interest rates result simply from an earlier installation of the heat pump and the higher CO<sub>2</sub> emissions at higher interest rates from a later installation.

As a further parameter, the supply temperature of the HP is assumed to be 67 °C instead of the 62 °C previously used ( $HPT_{max} 67\text{ °C}$ ). Through research and development, especially in refrigerants (cf. propane), HPs are now also available on the market that can reach up to 75 °C [69]. As the max. HP supply temperature increases from 62 to 67 °C, the switch from a bivalent to a mono-energetic system is accelerated (cf. Table 8). The envelope refurbishment does not change. As a consequence of the early mono-energetic system, the CO<sub>2</sub> emissions dropped to 7.25 kg/m<sup>2</sup>/a. Since the investment costs of the HP are assumed to be independent of the maximum possible supply temperature, the total costs also decrease with increasing temperatures. The influence of the requested high DHW temperature leads to a bivalent system in the case of HP supply temperatures of max. 62 °C. In this case, the gas condensing boiler is primarily required to support the DHW generation. Financially attractive mono-energetic systems therefore require lower DHW temperatures, e.g. by means of an ultrafiltration system or a HP with a supply temperature of at least 65 °C.

As a last parameter, the energy supply costs are increased by 50 % as they strongly depend on various technical as well as political framework conditions and are difficult to predict. In the case of the increased electricity purchase costs ( $E_{Price}+50\%$ ), the heat pump is installed with a delay and is significantly downsized. This leads to an increased use of the gas condensing boiler and results in higher emissions. The relevance of the electricity costs is also reflected in the high net present value with 13.25 €/m<sup>2</sup>/a. In the case of increased gas purchase costs ( $G_{Price}+50\%$ ), an even stronger influence on the system composition can be seen. Instead of a bivalent HP system, a mono-energetic HP system is now preferred. The high gas prices cause an immediate HP installation and lead to specific CO<sub>2</sub> emissions of 5.89 kg/m<sup>2</sup>/a, which is the lowest value of all cases investigated. An increase in both electricity and gas prices ( $EG_{Price}+50\%$ ) results in a reduction in the heating demand due to a better refurbishment level as well as an earlier start of refurbishment measures, as in the case of the windows. The parallel increase in energy costs does not change the system composition since the optimizer cannot switch to a cheaper energy source. Only the HP is installed ahead of time.

Table 8: Overview of the influence of different parameters on costs and CO<sub>2</sub> emission in relation to the optimized case optRR. Heat demand and size of heat generator of the year 2045 for comparison reasons.

case	spec. NPV	CO2	heat dem.	heat gen. [kW]	
	[€/m <sup>2</sup> /a]	[kg/m <sup>2</sup> /a]	[kWh/m <sup>2</sup> /a]	gas	hp
optRR	-12.44	8.94	53.3	7.5	17.5
0 €/tCO <sub>2</sub>	-12.27 (-1.4%)	10.77 (20.5%)	52.7	15.0	12.5
260 €/tCO <sub>2</sub>	-12.52 (0.6%)	8.53 (-4.6%)	53.3	7.5	17.5
Subsidy	-10.32 (-17.0%)	7.65 (-14.4%)	52.9	7.5	20.0
IR3%	-12.78 (2.7 %)	7.69 (-14.0%)	49.6	7.5	17.5
IR7%	-11.97 (-3.8%)	9.34 (4.5%)	54.0	7.5	17.5
HPT <sub>max</sub> 67 °C	-12.16 (-2.3%)	7.25 (-18.9%)	53.3	0.0	22.5
E <sub>Price</sub> +50 %	-13.25 (6.5%)	9.81 (9.7%)	51.4	12.5	15.0
G <sub>Price</sub> +50 %	-12.98 (4.3%)	5.89 (-34.1%)	53.3	0.0	20
EG <sub>Price</sub> +50%	-14.39 (15.7%)	6.73 (-24.7%)	49.6	7.5	17.5

Figure 6 compares the parameter variations listed in Table 8 for a better overview. This includes specific data on the annual NPV and CO<sub>2</sub> emissions per square meter of heated building area over the entire period under consideration. Likewise, the share of the HP power relative to the total heating power and the specific heating demand for the year 2045 are shown graphically. In addition, the time of the HP installation as well as the HP fraction (related to the year 2045) are also shown.

Based on the used cost assumptions for the insulation of the building envelope, the optimizer chooses a very narrow target corridor for the heating demand between 49 and 54 kWh/(m<sup>2</sup>a). Only a minor impact from energy costs and interest rates can be observed. With few exceptions, the percentage share of the HP power is about 70 %. Only the high electricity purchase costs (55 % HP share), no CO<sub>2</sub> pricing (45 % HP share) and high HP supply temperature as well as high gas prices (100% HP share) deviate noticeably from

this. The period of the HP installation is also very narrow, with a span of 7 years (2021-2028). Subsidies, low interest rates and high gas prices have a positive influence on early HP installation, while high electricity purchase costs or the lack of CO<sub>2</sub> pricing have a negative influence. With regards to the specific net present values, the strong influence of the subsidies stands out, as well as the high combined energy prices. The remaining scenarios have NVPs that are very close to each other, ranging from 11.5 to 12.5 €/m<sup>2</sup>a). In terms of CO<sub>2</sub> emissions, however, a wider range of 6 to 10 kg/(m<sup>2</sup>a) is observed. Since the refurbishment level hardly differs between the scenarios, an early installation of HP (high gas prices, subsidies, low interest rates) and a large share of HP coverage (high HP supply temperatures) have a beneficial effect. Consequently, a later HP installation (no CO<sub>2</sub> pricing, high electricity purchase costs) is counterproductive. Due to the almost identical HP share of the scenarios, the HP fraction is also very similar between approx. 82-84 %. Only the high HP supply temperature and the possibility of DHW generation via HP reach a value of 97 %. In contrast, the scenarios with no CO<sub>2</sub> pricing and high electricity costs show a HP fraction of less than 80 %.

Note that all cases use brine heat pumps – air source heat pumps are not selected despite the option of the optimizer to select this alternative system. This is due to the fact that, over the entire observed period, the net present value of the brine heat pump is more economic than that of an air source heat pump.

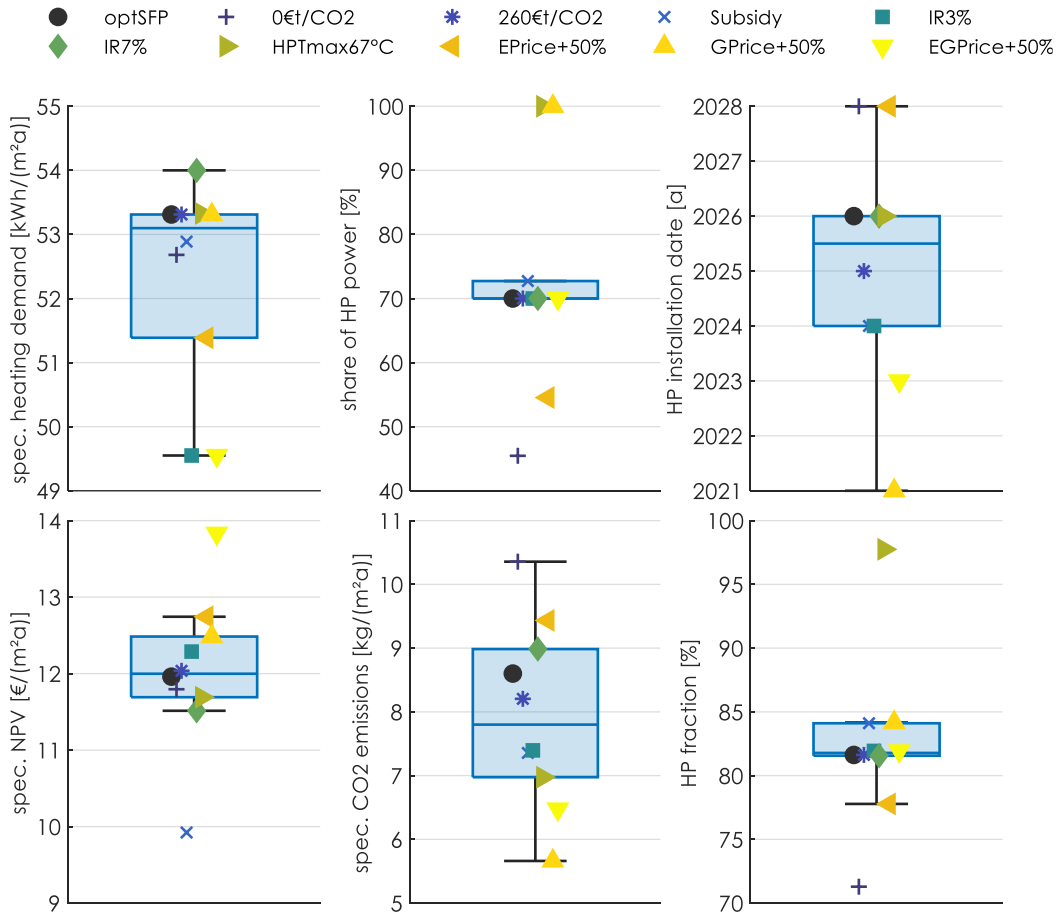


Figure 6: Comparison of the investigated parameter variations with regard to the spec. heating demand, share of HP power, HP installation date, spec. NPV, spec. CO<sub>2</sub> emissions and HP fraction. Results are valid for degree of freedom as in case *optRR* (box plot contains the median (line inside box), the 0.25 and 0.75 quantile (bottom and top edge of box) with the interquartile range (iqr) as the distance between the two, outliers (distance > 1.5 iqr from the 0.25 or 0.75 quantile) as well as min. and max. values that are not outliers and connected with a whisker to the 0.25 or 0.75 quantile)

#### 4.4. Robustness of refurbishment roadmaps concerning the initial state of the building

Buildings differ with respect to their geometric dimensions, thermal characteristics, age class and heat supply systems. To study their influence on the robustness of the refurbishment roadmap, the optimization method is applied to different building sizes and ages. A small (SMH-70), medium (MMH-70) and large multi-family house (LMH-70) built in 1970 and a medium multi-family house (MMH-90) built in 1990 are compared for this purpose (cf. Table 13 and Table 14). In all cases, the initial heating supply system is assumed to be a gas condensing boiler.

Figure 7 shows the specific heat demand, specific costs, HP share and specific CO<sub>2</sub> emissions for the four different building classes. The differences can be attributed to different starting refurbishment levels, decreasing area-specific costs, or varying surface-to-volume ratios. All comparison parameters decrease

with increasing building size, except for the share of heat pumps. The MMH-90 building will be refurbished later due to its newer construction age. This leads to lower refurbishment and maintenance costs, but higher heat demands and CO<sub>2</sub>-emissions have to be accepted.

Despite the different initial conditions, the optimizer chooses a similar heat supply system, which consists of a bivalent heat pump with a gas boiler. The medium share of HP power ranges between 60 % of a small MFH and 80 % of a large MFH. The increasing share of HPs in larger MFH is due to the fast decreasing performance-specific costs of the HP and the decreasing share of domestic hot water due to lower circulation losses.

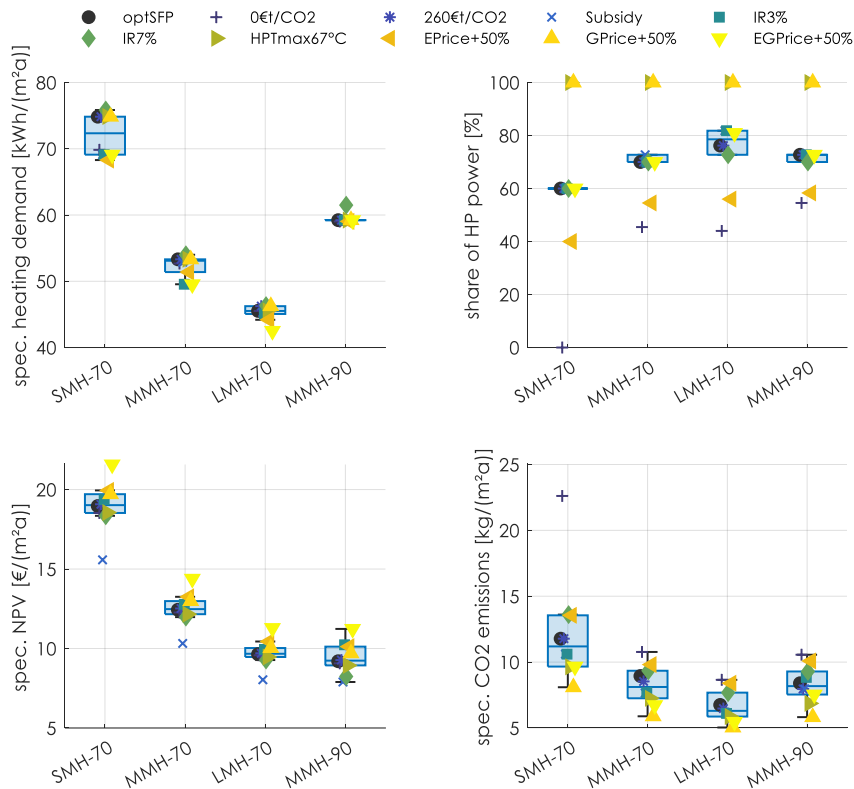


Figure 7: Comparison of the investigated parameter variations with regard to the spec. heating demand, share of HP power, spec. NPV and spec. CO<sub>2</sub> emissions. Results are valid for degree of freedom as in case *optRR* (box plot contains the median (line inside box), the 0.25 and 0.75 quantile (bottom and top edge of box) with the interquartile range (iqr) as the distance between the two, outliers (distance > 1.5 iqr from the 0.25 or 0.75 quantile) as well as min. and max. values that are not outliers and connected with a whisker to the 0.25 or 0.75 quantile)

## 5. Discussion

A mathematical optimization approach is needed for a cost-optimal selection of the right measures at the right time, as section 4.2 demonstrates in comparison to non-optimized or only partially optimized cases. The overall costs decrease with the number of degrees of freedom of the optimizer. The reason for using an optimization is the large number of possible combinations, since the solution space consists of the different refurbishment times, the number of possible technologies and thermal insulation measures, and their respective specifications. Furthermore, the components influence each other and there are time-varying parameters (e.g. energy prices). For example, the insulation of the building envelope reduces the heating load, which in return lowers the supply temperature and increases the efficiency of the gas condensing boiler or heat pump. Consequently, all optimization parameters must be considered in the overall context.

The identified refurbishment roadmaps show a high robustness against different influencing factors (CO<sub>2</sub> pricing, subsidies, interest rates, max. HP supply temperature and electricity purchase costs) as shown in section 4.3. Referring to the investigated medium-sized multi-family building from 1970, a robust refurbishment roadmap with a brine-HP installation between the years 2021 and 2028 results. The heat supply system is designed as a bivalent system with a heat pump share of 70 %. The refurbishment of the building envelope aims at a heating demand of approx. 50 kWh/m<sup>2</sup>/a and always takes place at the end of the technical lifetime of the building components. An exception is the floor insulation, which is being refurbished ahead of schedule. In the case of high energy prices, this also applies to the windows.

The refurbishment roadmaps are also robust against different initial conditions of building geometry and age class. The optimum heat supply system is consistently given by a bivalent HP system with a share of HP power between 60 - 80 % (cf 4.4).

Based on the identified refurbishment roadmaps, the following general conclusions can be drawn in the context of the assumed framework:

- Heat pumps play a central role in reducing heat production costs and emissions. In the majority of the investigated scenarios, a bivalent system is necessary due to the high DHW supply temperatures. When differentiating between outdoor air and ground-source HP, the latter has a slight monetary advantage. However, this is strongly linked to the environmental conditions, e.g. general drilling permission (keyword: drinking water protection area) or assumed thermal conductivity of the underground.
- Under the current assumptions, bivalent systems are superior to both the gas condensing boiler and the mono-energetic HP systems in terms of costs. However, mono-energetic systems are essential to achieve the targeted CO<sub>2</sub> reductions. Possible measures to increase the share of mono-energetic systems include increasing the maximum HP supply temperature or reducing the required DHW supply temperature, reducing investment costs through subsidies and reducing electrical energy costs.

- Under both economic and ecological considerations, the system switch to a bivalent HP system offers a significantly greater savings effect than a major building envelope refurbishment. From an economic point of view, the heating demand settles around 50 kWh/(m<sup>2</sup>a) (cf. Figure 6), which corresponds to a low-energy house standard. The increased insulation towards the passive-house standard is not refinanced by the heating energy saved.

Within the scope of this analysis, the focus is placed on heating-dominated climates with corresponding building physics. In other locations, the optimization might yield differing results.

## 6. Conclusions

The presented work describes the development of a methodology for the calculation of cost-optimized refurbishment roadmaps for multi-family buildings with a focus on heat pumps. The novel optimization method consists of a dynamic thermal building and system simulation coupled with a particle swarm optimization. The objective is the identification of when and how should which component be refurbished in order to supply a building with heat at an optimal cost. In addition to the insulation level of the building envelope and the heating power for the heat supply, it also determines the time of implementation of each component. The U-value of five envelope components (window, wall, ceiling, floor, roof), the type and power of three heat generator technologies (gas boiler, air-source heat pump, ground-source heat pump) and their corresponding implementation dates comprise the search state and are subject to the optimization method. Furthermore, coupling effects between refurbishment measures and heat supply technologies are taken into account, such as the dependence of the coefficient of performance on the supply temperature, which in turn is a function of the insulation standard. Through the individual settings of the initial state and restrictions of the solution space (e.g. no ground source heat pump because of water protection area etc., compliance with certain CO<sub>2</sub> limits), an individual solution customized to the building is possible.

The newly developed methodology for optimizing the refurbishment roadmap is successfully demonstrated using a typical German multi-family building as an example. The added value of the complex approach is demonstrated by varying the degrees of freedom in the search space for the optimizer. The roadmap is thereby independent of subjective expert knowledge, takes into account the future development of costs and specific CO<sub>2</sub> emissions and allows a free choice of implementation dates. Depending on the number of variable parameters, the optimization enables cost savings of between 6 and 16 % and CO<sub>2</sub> savings of between 6 and 59 % over the period under consideration.

In addition, the robustness of the refurbishment roadmap concerning the sensitivity of selected parameters and initial conditions is discussed. The CO<sub>2</sub> savings increase with a longer operation period of the heat pump application and the amount of heat generated by it. In order to achieve a climate-neutral building stock, mono-energetic systems should therefore be aimed at in the long term. Under the assumed boundary conditions (costs, emissions, building type, construction year, etc.) and as a result of the previous investigations, the following conclusions can be drawn:

- The cost-optimal refurbishment level is a low-energy house standard with an average of approx. 45-60 kWh/a/m<sup>2</sup> for medium and large multi-family houses and about 70 kWh/a/m<sup>2</sup> for small multi-family houses.
- A significant CO<sub>2</sub> reduction can only be achieved through the use of heat pumps
- A cost-optimized heat supply system uses a bivalent system consisting of a gas condensing boiler and a brine HP. The share of heat pump power in the bivalent system is approx. 60-80%.

Further improvements of the optimization model could include, for example, the addition of more technologies (district heating, photovoltaics, wood pellet heating), implementation of cooling systems, the analysis of more building types and building age classes in different climates and from various countries, as well as a more realistic representation of the internal cash flow.

### **Acknowledgements**

We gratefully acknowledge financial support of the German Federal Ministry for Economic Affairs and Energy (BMWi) due to an enactment of the German Bundestag under grant numbers 03SBE0001 (LowEx-Bestand).

## Nomenclature

Symbol	Description	Unit
$\vec{g}_{best}$	global memory	
$\vec{l}_{best}$	local memory	
$\vec{v}$	velocity vector	
$\vec{x}$	position vector	
a, b	regression coefficients	
AHP	air heat pump	
BHP	brine heat pump	
$c_1$	cognitivte factor	
$c_2$	social factor	
COP	coefficient of performance	
DHW	domestic hot water	
ETICS	external thermal insulation composite system	
GEG	German building energy law	
HP	heat pump	
iqr	interquartile range	
LCOH	levelized cost of heat	€/kWh
LMH	large multi-family house	
MFH	multi-family house	
MMH	medium multi-family house	
mro	maintenance, repair and operation costs	€
$n_G$	number of generations	
$n_p$	population size	
NPV	net present value	
$p_{CO_2}$	CO2 pricing	€/tCO <sub>2</sub>
PSO	particle swarm optimization	
q	interest rate	%
r	inflation rate	%
$r_{1,2}$	random numbers between [0,1]	
rv	residual value	€
SH	space heating	
SMH	small multi-family house	
T	period under consideration	a
$T_{HP}$	max. heat pump supply temperature	°C
TIG	thermal insulation glazing	
z	investment costs	€
$\omega_{1,2}$	inertia weight	

## References

- [1] H.-M. Henning, A. Palzer, Was kostet die Energiewende?: Wege zur Transformation des deutschen Energiesystems bis 2050, Freiburg, 2015.
- [2] A. Breitkopf, Anteil der Wärmepumpen im Neubau in Deutschland in den Jahren 2000 bis 2020, 2021. <https://de.statista.com/statistik/daten/studie/237364/umfrage/bedeutung-der-waermepumpen-im-neubau-in-deutschland/> (accessed 4 January 2022).
- [3] Destatis, Baufertigstellungen neuer Gebäude: Deutschland, Jahre, Gebäudeart, Energieverwendung, Energieart: Ergebnis 31121-0004, 2021. <https://www-genesis.destatis.de/genesis/online?operation=abrufabelleBearbeiten&levelindex=2&levelid=1641308231873&auswahloperation=abrufabelleAuspraegungAuswaehlen&auswahlverzeichnis=ordnungssstruktur&auswahlziel=werteabruf&code=31121-0004&auswahltext=&werteabruf=Werteabruf#abreadcrumb> (accessed 4 January 2022).
- [4] BWP, Positives Signal für den Klimaschutz: 40 Prozent Wachstum bei Wärmepumpen, 2021. <https://www.waermepumpe.de/presse/pressemitteilungen/details/positives-signal-fuer-den-klimaschutz-40-prozent-wachstum-bei-waermepumpen/#content> (accessed 2 March 2021).
- [5] BDH, Trotz Corona: Deutsche Heizungsindustrie schaffte 2020 ein robustes Wachstum von 3,1%, 2021. <https://www.baulinks.de/webplugin/2021/0195.php4> (accessed 4 January 2022).
- [6] Fraunhofer IWES/IBP, Wärmewende 2030: Schlüsseltechnologien zur Erreichung der mittel- und langfristigen Klimaschutzziele im Gebäudesektor, Berlin, 2017.
- [7] P. Sterchele, J. Brandes, J. Heilig, D. Wrede, C. Kost, T. Schlegl, A. Bett, H.-M. Henning, Wege zu einem klimaneutralen Energiesystem: Die deutsche Energiewende im Kontext gesellschaftlicher Verhaltensweisen, Freiburg im Breisgau, 2020.
- [8] J. Brandes, M. Haun, D. Wrede, P. Jürgens, C. Kost, H.-M. Henning, Wege zu einem klimaneutralen Energiesystem: Die deutsche Energiewende im Kontext gesellschaftlicher Verhaltensweisen, Freiburg im Breisgau, 2021.
- [9] Z. Ma, P. Cooper, D. Daly, L. Ledo, Existing building retrofits: Methodology and state-of-the-art, *Energy and Buildings* 55 (2012) 889–902. <https://doi.org/10.1016/j.enbuild.2012.08.018>.
- [10] A.-T. Nguyen, S. Reiter, P. Rigo, A review on simulation-based optimization methods applied to building performance analysis, *Applied Energy* 113 (2014) 1043–1058.
- [11] I. Costa Carrapiço, R. Raslan, J.N. González, A systematic review of genetic algorithm-based multi-objective optimisation for building retrofitting strategies towards energy efficiency, *Energy and Buildings* 210 (2020). <https://doi.org/10.1016/j.enbuild.2019.109690>.
- [12] G. Verbeeck, H. Hens, Energy savings in retrofitted dwellings: economically viable?, *Energy and Buildings* 37 (2005) 747–754. <https://doi.org/10.1016/j.enbuild.2004.10.003>.
- [13] O. Kah, W. Feist, Wirtschaftlichkeit von Wärmedämm- Maßnahmen im Gebäudebestand 2005,

Darmstadt, 2005.

- [14] A. Enseling, E. Hinz, *Wirtschaftlichkeit energiesparender Maßnahmen im Bestand vor dem Hintergrund der novellierten EnEV*, first. Aufl., Institut Wohnen und Umwelt, Darmstadt, 2008.
- [15] A. Enseling, E. Hinz, M. Vaché, *Akteursbezogene Wirtschaftlichkeitsberechnungen von Energieeffizienzmaßnahmen im Bestand*, Darmstadt, 2013.
- [16] M. Almeida, M. Ferreira, Cost effective energy and carbon emissions optimization in building renovation (Annex 56), *Energy and Buildings* 152 (2017) 718–738. <https://doi.org/10.1016/j.enbuild.2017.07.050>.
- [17] S.-I. Gustafsson, Mixed integer linear programming and building retrofits, *Energy and Buildings* 28 (1998) 191–196. [https://doi.org/10.1016/S0378-7788\(98\)00019-X](https://doi.org/10.1016/S0378-7788(98)00019-X).
- [18] S.-I. Gustafsson, Sensitivity analysis of building energy retrofits, *Applied Energy* 61 (1998) 13–23. [https://doi.org/10.1016/S0306-2619\(98\)00032-4](https://doi.org/10.1016/S0306-2619(98)00032-4).
- [19] F. Pernodet, H. Lahmidi, P. Michel, Use of genetic algorithms for multicriteria optimization of building refurbishment, in: *Eleventh International IBPSA Conference*, Glasgow; Scotland, 2009, pp. 188–195.
- [20] C. Diakaki, E. Grigoroudis, N. Kabelis, D. Kolokotsa, K. Kalaitzakis, G. Stavrakakis, A multi-objective decision model for the improvement of energy efficiency in buildings, *Energy* 35 (2010) 5483–5496. <https://doi.org/10.1016/j.energy.2010.05.012>.
- [21] Y. Fan, X. Xia, A Multi-objective Optimization Model for Building Envelope Retrofit Planning, *Energy Procedia* 75 (2015) 1299–1304. <https://doi.org/10.1016/j.egypro.2015.07.193>.
- [22] Y. Fan, X. Xia, A multi-objective optimization model for energy-efficiency building envelope retrofitting plan with rooftop PV system installation and maintenance, *Applied Energy* 189 (2017) 327–335. <https://doi.org/10.1016/j.apenergy.2016.12.077>.
- [23] R. Kunze, *Techno-ökonomische Planung energetischer Wohngebäudemodernisierungen Ein gemischt-ganzzahliges lineares Optimierungsmodell auf Basis einer vollständigen Finanzplanung*, KIT Scientific Publishing, 2016.
- [24] K. Peippo, P.D. Lund, E. Vartiainen, Multivariate optimization of design trade-offs for solar low energy buildings, *Energy and Buildings* 29 (1999) 189–205. [https://doi.org/10.1016/S0378-7788\(98\)00055-3](https://doi.org/10.1016/S0378-7788(98)00055-3).
- [25] T.R. Nielsen, *Optimization of buildings with respect to energy and indoor environment*. Dissertation, 2003.
- [26] R. Almeida, V. Freitas, Multi-objective optimization for school buildings retrofit combining artificial neural networks and life cycle cost, *ESTGV - DEC - Documentos de congressos* (2013).
- [27] E. Asadi, M.G.d. Silva, C.H. Antunes, L. Dias, L. Glicksman, Multi-objective optimization for building retrofit: A model using genetic algorithm and artificial neural network and an application, *Energy and Buildings* 81 (2014) 444–456. <https://doi.org/10.1016/j.enbuild.2014.06.009>.

- [28] F. Shadram, S. Bhattacharjee, S. Lidelöw, J. Mukkavaara, T. Olofsson, Exploring the trade-off in life cycle energy of building retrofit through optimization, *Applied Energy* 269 (2020) 115083. <https://doi.org/10.1016/j.apenergy.2020.115083>.
- [29] S. Cypra, Auswirkungen von Energieeffizienzsertifikaten auf Investitionsentscheidungen im Wohnungsbau. Zugl.: Karlsruhe, Univ., Diss., 2009, KIT Scientific Publishing, Karlsruhe, 2010.
- [30] G. Kumbaroğlu, R. Madlener, Evaluation of economically optimal retrofit investment options for energy savings in buildings, *Energy and Buildings* 49 (2012) 327–334. <https://doi.org/10.1016/j.enbuild.2012.02.022>.
- [31] Deutsche Energie-Agentur, Institut für Energie- und Umweltforschung, Passivhaus Institut, Handbuch für Energieberaterinnen und Energieberater: Anleitung mit Tipps und Tricks zur Umsetzung, Berlin, 2020.
- [32] A. Hoier, H. Erhorn, Energetische Gebäudesanierung in Deutschland: Studie Teil I: Entwicklung und energetische Bewertung alternativer Sanierungsfahrpläne, Stuttgart, 2013.
- [33] H. Nymoen, K. Graf, E. Niemann, M. Kröber, Klimaneutral Wohnen: Klimaschutz im Wärmemarkt: Wie können wir Klimaneutralität im Bereich der Wohngebäude erreichen?, Berlin, 2021.
- [34] D. Fischer, synPRO, 2022. <https://energysolutions.tools/elink-tools/synpro/> (accessed 5 January 2022).
- [35] Deutsches Institut für Normung e.V., Energieeffizienz von Gebäuden: Berechnung des Energiebedarfs für Heizung und Kühlung, Beuth Verlag GmbH, Berlin ICS 91.140.10, 2008.
- [36] R. Walraven, Calculating the position of the sun, *Solar Energy* 20 (1978) 393–397. [https://doi.org/10.1016/0038-092X\(78\)90155-X](https://doi.org/10.1016/0038-092X(78)90155-X).
- [37] V. Quaschnig, Regenerative Energiesysteme: Technologie – Berechnung – Klimaschutz, tenth., aktualisierte und erweiterte Auflage, Hanser, München, 2019.
- [38] M. Lämmle, C. Bongs, J. Wapler, D. Günther, S. Hess, M. Kropp, S. Herkel, Performance of air and ground source heat pumps retrofitted to radiator heating systems and measures to reduce space heating temperatures in existing buildings, *Energy* 242 (2022) 122952. <https://doi.org/10.1016/j.energy.2021.122952>.
- [39] DVGW Deutscher Verein des Gas- und Wasserfaches e. V., Arbeitsblatt W 551: Trinkwassererwärmungs- und Trinkwasserleitungsanlagen - Technische Maßnahmen zur Verminderung des Legionellenwachstums - Planung, Errichtung, Betrieb und Sanierung von Trinkwasser-Installationen, Beuth Verlag GmbH, Berlin, 2004.
- [40] TU Berlin, StorageStandard: Modell eines Warmwasserspeichers, Berlin, 2002.
- [41] H. Drück, Multiport Store - Model: Type 340, Stuttgart, 2006.
- [42] U. Eicker, Solare Technologien für Gebäude: Grundlagen und Praxisbeispiele, second., vollständig überarbeitete Auflage, Vieweg+Teubner Verlag / Springer Fachmedien Wiesbaden GmbH Wiesbaden, Wiesbaden, 2012.

- [43] T. Afjei, M. Wetter, Compressor heat pump including frost and cycle losses: Model description and implementing into TRNSYS, Luzern, 1997.
- [44] Dimplex, LIK 12TU: Kompakte Luft/Wasser-Wärmepumpe zur Innenaufstellung, 2022. <https://dimplex.de/dimplex/waermepumpen/li-lik/lik12tu> (accessed 1 March 2022).
- [45] Stiebel Eltron, WPF 27: Sole-Wasser-Wärmepumpen, 2022. [https://www.stiebel-eltron.de/de/home/produkte-loesungen/erneuerbare\\_energien/waermepumpe/sole-wasser-waermepumpen/wpf-20-66/wpf-27.html](https://www.stiebel-eltron.de/de/home/produkte-loesungen/erneuerbare_energien/waermepumpe/sole-wasser-waermepumpen/wpf-20-66/wpf-27.html) (accessed 1 March 2022).
- [46] Viessmann, Technikal Data Manual: Vitocrossal 200, 2018.
- [47] Verein deutscher Ingenieure, Thermische Nutzung des Untergrunds: Erdgekoppelte Wärmepumpenanlagen, Beuth Verlag GmbH, Berlin 27.080, 2019.
- [48] R. Königsdorff, Oberflächennahe Geothermie für Gebäude: Grundlagen und Anwendungen einer zukunftsfähigen Heizung und Kühlung, Fraunhofer IRB Verlag, Stuttgart, 2011.
- [49] Verein deutscher Ingenieure, Wirtschaftlichkeit gebäudetechnischer Anlagen: Grundlagen und Kostenberechnung, Beuth Verlag GmbH, Berlin 91.140.01, 2012.
- [50] Europäische Zentralbank, EZB-Rat verabschiedet neue geldpolitische Strategie, 2021. <https://www.ecb.europa.eu/press/pr/date/2021/html/ecb.pr210708~dc78cc4b0d.de.html> (accessed 5 October 2021).
- [51] BundesBauBlatt, Wohnungsunternehmen erzielen mehr Rendite durch Modernisierung: Besser energieeffizient „aufpolieren“ als kaufen, 2015. [https://www.bundesbaublatt.de/artikel/bbb\\_Wohnungsunternehmen\\_erzielen\\_mehr\\_Rendite\\_durch\\_Modernisierung\\_2367550.html](https://www.bundesbaublatt.de/artikel/bbb_Wohnungsunternehmen_erzielen_mehr_Rendite_durch_Modernisierung_2367550.html) (accessed 29 October 2021).
- [52] D. Goldberg, Genetic Algorithms in Search, Optimization, and Machine Learning, Addison-Wesley Publishing Company, Inc., 1989.
- [53] M. Biberacher, Modelling and optimisation of future energy systems using spatial and temporal methods. Dissertation, Augsburg, 2004.
- [54] D. Schröder, M. Buss, Intelligente Verfahren: Identifikation und Regelung Nichtlinearer Systeme, secondnd ed., Vieweg, Berlin, Heidelberg, 2017.
- [55] A. Schumacher, Optimierung mechanischer Strukturen: Grundlagen und industrielle Anwendungen, second., aktualisierte und erw. Aufl., Springer Vieweg, Berlin, 2013.
- [56] J. Kennedy, R. Eberhart, Particel Swarm Optimization, in: Proceedings of the IEEE International Conference on Neural Networks, University of Western Australia; Perth, 1995, pp. 1942–1948.
- [57] R. Eberhart, J. Kennedy, A new optimizer using particle swarm theory, in: Proceedings of the Sixth International Symposium on Micro Machine and Human Science, Nagoya Municipal Industrial Research Institute, 1995, pp. 39–43.
- [58] D. Bratton, J. Kennedy, Defining a Standard for Particle Swarm Optimization, in: 2007 IEEE Swarm Intelligence Symposium, Honolulu, HI, USA, IEEE, 01.04.2007 - 05.04.2007, pp. 120–127.

- [59] Y. Shi, R. Eberhart, Empirical study of particle swarm optimization, in: Proceedings of the 1999 Congress on Evolutionary Computation-CEC99 (Cat. No. 99TH8406), 1999, pp. 1945–1950.
- [60] A. Ratnaweera, S. Halgamuge, H. Watson, Self-Organizing Hierarchical Particle Swarm Optimizer With Time-Varying Acceleration Coefficients, IEEE Transaction on Evolutionary Computation 8 (2004) 240–255.
- [61] S. Helwig, Particle Swarms for Constrained Optimization: Partikelschwärme für Optimierungsprobleme mit Nebenbedingungen. Dissertation, Erlangen, 2010.
- [62] N. Diefenbach, Basisdaten für Hochrechnungen mit der Deutschen Gebäudetypologie des IWU: Neufassung Oktober 2013, Darmstadt, 2013.
- [63] DIN Deutsches Institut für Normung e.V., Energetische Bewertung von Gebäuden – Berechnung des Nutz-, End- und Primärenergiebedarfs für Heizung, Kühlung, Lüftung, Trinkwarmwasser und Beleuchtung: Teil 10: Nutzungsrandbedingungen, Klimadaten, Beuth Verlag GmbH, Berlin 91.120.10, 2018.
- [64] Verein deutscher Ingenieure, Wärmeschutz und Energie-Einsparung in Gebäuden: Berechnung des Jahresheizwärme- und des Jahresheizenergiebedarfs, Beuth, Berlin 91.120.10, 2003.
- [65] B. Ebert, Systematische Analyse der Mehrfamilien-Bestandsgebäude: Bericht zu AP 1.1, Karlsruhe, 2020.
- [66] DIN Deutsches Institut für Normung e.V., Wärmeschutz und Energie-Einsparung in Gebäuden: Teil 4: Wärme- und feuchteschutztechnische Bemessungswerte, Beuth Verlag GmbH, Berlin 91.120.10, 2017.
- [67] Deutsches Institut für Normung e.V., Energetische Bewertung von Gebäuden - Energiebedarf für Heizung und Kühlung, Innentemperaturen sowie fühlbare und latente Heizlasten: Teil 1: Berechnungsverfahren (ISO 52016-1:2017), Beuth Verlag GmbH, Berlin 91.120.10; 91.140.10, 2018.
- [68] BAFA, Förderübersicht: Bundesförderung für effiziente Gebäude (BEG), 2021. [https://www.bafa.de/SharedDocs/Downloads/DE/Energie/beg\\_em\\_foerderuebersicht.pdf?\\_\\_blob=publicationFile&v=5](https://www.bafa.de/SharedDocs/Downloads/DE/Energie/beg_em_foerderuebersicht.pdf?__blob=publicationFile&v=5) (accessed 17 January 2022).
- [69] M. Miara, Wärmepumpen im Bestand, Teil 1: Auch unsaniert passt die Vorlauftemperatur, TGA Fachplaner (2021).
- [70] E. Hinz, Kosten energierelevanter Bau- und Anlagenteile bei der energetischen Modernisierung von Altbauten: Endbericht, first. Auflage, Institut Wohnen und Umwelt, Darmstadt, 2015.
- [71] B. Oschatz, J. Rosenkranz, S. Arzt, A. Steuerlein, Kosten energierelevanter Bau- und technischer Anlagenteile bei der energetischen Sanierung von Nichtwohngebäuden/Bundesliegenschaften, Bonn, 2014.
- [72] F. Bräuer, B. Rodenbücher, K. Scharf, R. Vollmer, R. Eberle, J. Wapler, C. Bongs, F. Schmidt, M. Ruppert, S. Hess, Techno-ökonomische Analyse von Sanierungspaketen aus Gebäudehülle und LowEx-Systemen: Projekt LowEx-Bestand Analyse - Bericht zu AP 5.3, 2022.

- [73] A. Breitkopf, Baupreisindex: Preisentwicklung für Bauleistungen an Wohngebäuden bis 2020, 2021. <https://de.statista.com/statistik/daten/studie/70134/umfrage/baupreisindex-fuer-wohngebaeude-in-deutschland/> (accessed 4 October 2021).
- [74] Bundesnetzagentur, Monitoringbericht 2020: Monitoringbericht gemäß § 63 Abs. 3 i. V. m. § 35 EnWG und § 48 Abs. 3 i. V. m. § 53 Abs. 3 GWB, Bonn, 2021.
- [75] J. Wagner, R. Madlener, O. Hennes, J. Zinke, S. Jeddi, H. Schmitz, S. Wolff, Auswirkungen von CO<sub>2</sub>-Preisen auf den Gebäude-, Verkehrs- und Energiesektor: Kurzstudie, Essen, 2019.
- [76] U. Fritsche, H.-W. Greß, Der nichterneuerbare kumulierte Energieverbrauch und THG-Emissionen des deutschen Strommix im Jahr 2018 sowie Ausblicke auf 2020 bis 2050: Bericht für die HEA - Fachgemeinschaft für effiziente Energieanwendung e.V., Darmstadt, 2019.
- [77] IINAS, GEMIS (Globales Emissions-Modell integrierter Systeme): Version 5.0, 2018. <http://iinas.org/gemis-de.html>.

## Appendix

Table 9: Regression coefficients for spec. cost formulas [€/m<sup>2</sup>] for the building envelope components according to [70–72]<sup>†</sup>

component	description	formula	
		a [€/m <sup>2</sup> ]	b [-]
$y = (a \cdot x^b)$ [€/m <sup>2</sup> ]			
window	2-TIG <sup>1)</sup> (U value = 1.9 W/m <sup>2</sup> K)	414.18	-0.212
	2- TIG (U value = 1.3 W/m <sup>2</sup> K)	467.23	-0.232
	3- TIG (U value = 1.0 W/m <sup>2</sup> K)	541.27	-0.231
	3- TIG (U value = 0.8 W/m <sup>2</sup> K)	742.75	-0.208
$y = (a \cdot x + b)$ [€/m <sup>2</sup> ]		a [€/m <sup>2</sup> ]	b [€/m <sup>2</sup> ]
external wall	external thermal insulation composite system	281.1	102.68
floor	bottom side / unclad	183.2	45.504
ceiling	walkable	214	28.67
roof	pitched roof	279	158.9

<sup>1)</sup> TIG = thermal insulation glazing

Table 10: Regression coefficients for specific cost formulas [€/kW] for the heat generation components according to [72]

component	description	formula	
		a [€/kW]	b [-]
$y = (a \cdot x^b)$ [€/kW]			
gas boiler		1045.6	-0.415
outdoor air HP		5670.1	-0.537
brine HP	without probe drilling	3693.3	-0.578
$y = (a \cdot x + b)$ [€]		a [€/m]	b [€]
probe <sup>1)</sup>	costs for probe field (up to 160 m depth)	90	3000

<sup>1)</sup> Own evaluation of cost offers

<sup>†</sup> Adjusted to the development of the construction price index for construction services on residential buildings between 2015 with index 100 and 2020 with index 116.4 [73].

Table 11: Heat pump electricity price and gas price for the three price scenarios (without CO<sub>2</sub> pricing, final price 180 €/tCO<sub>2</sub> in 2050, final price 260 €/tCO<sub>2</sub> in 2050) with the standard case for all simulations of 180 €/tCO<sub>2</sub> [72]

year	heat pump electricity price <sup>1)</sup> in €/kWh			natural gas price in €/kWh		
	without CO <sub>2</sub> - price	180 €/tCO <sub>2</sub> in 2050	260 €/tCO <sub>2</sub> in 2050	without CO <sub>2</sub> - price	180 €/tCO <sub>2</sub> in 2050	260 €/tCO <sub>2</sub> in 2050
2020 <sup>2)</sup>		0.2358			0.0631	
2030 <sup>3)</sup>	0.2276	0.1920	0.1920	0.0879	0.1091	0.1132
2040 <sup>4)</sup>	0.2154	0.1952	0.1956	0.0915	0.1289	0.1405
2050	0.2031	0.1984	0.1992	0.0950	0.1486	0.1678

<sup>1)</sup> heat pump electricity tariff 78.2% of regular household electricity price [74]

<sup>2)</sup> values for the year 2020 [74]

<sup>3)</sup> values for the year 2030 / 2050 with factor 1.047 (electricity) and 1.0106 (gas) from 2017 to 2020 [75]

<sup>4)</sup> linear interpolation

Table 12: CO<sub>2</sub> and primary energy factors for electricity [76] and natural gas [77] locally at the consumer [72]

year	electricity		natural gas <sup>1)</sup>	
	CO <sub>2</sub> emissions [g/kWh]	primary energy factor [-]	CO <sub>2</sub> emissions [g/kWh]	primary energy factor [-]
2020	402.9	1.47	200.8	1.07
2030	193.0	0.65	183.9	0.97
2040 <sup>3)</sup>	107.1	0.35	175.2	0.92
2050	21.1	0.05	166.4	0.87

<sup>1)</sup> based on gross calorific value (original source specifies net calorific value – therefore here: conversion factor of 1.11)

<sup>2)</sup> consideration of power-to-gas: 2020: 3.4 %, 2030: 14.1 %, 2050: 25.0 %

<sup>3)</sup> linear interpolation

Table 13: Dimension of the investigated small, medium and large multi-family buildings

parameter	value / comment		
	small MFH (SMH)	medium MFH (MMH)	large MFH (LMH)
number of full storeys	2	3	5
number of apartments	4	12	30
number of staircases	1	2	3
cellar & attic	available and non-heated		
building orientation	north-south (gable side)		
building dimensions	11.9 m x 16.1 m	11.9 m x 32.1 m	11.9 m x 48.1 m
storey height	2.75 m		
clear ceiling height	2.55 m		
conditioned living space per apartment	75.7 m <sup>2</sup>		
net floor space	323.2 m <sup>2</sup>	969.5 m <sup>2</sup>	2423.7 m <sup>2</sup>

Table 14: Initial condition of the relevant optimization parameters in 2020 of the investigated building age class of 1990

component	initial value	technical lifetime	installation date
window	3.20 W/(m <sup>2</sup> K)	30 a	1990
exterior wall	0.66 W/(m <sup>2</sup> K)	40 a	1990
top floor ceiling	0.38 W/(m <sup>2</sup> K)	60 a	1990
bottom floor	0.58 W/(m <sup>2</sup> K)	60 a	1990
roof	1.27 W/(m <sup>2</sup> K)	50 a	1990
gas condensing boiler	52.5 kW	20 a	2010